PHYSICAL REVIEW
LETTERS

VOLUME 86 | 19 MARCH 2001 | NUMBER 12

Shape of the Quantum Diffusion Front

Jianxin Zhong,[1,2,3] R. B. Diener,[1] Daniel A. Steck,[1] Windell H. Oskay,[1] Mark G. Raizen,[1] E. Ward Plummer,[2,4] Zhenyu Zhang,[2,4] and Qian Niu[1,2]

[1]*Department of Physics, University of Texas at Austin, Austin, Texas 78712*
[2]*Solid State Division, Oak Ridge National Laboratory, Oak Ridge, Tennessee 37831*
[3]*Department of Physics, Xiangtan University, Hunan 411105, China*
[4]*Department of Physics, University of Tennessee, Knoxville, Tennessee 37996*
(Received 27 July 2000)

We show that quantum diffusion has well-defined front shape. After an initial transient, the wave packet front (tails) is described by a stretched exponential $P(x,t) = A(t)\exp(-|x/w|^{\gamma})$, with $1 < \gamma < \infty$, where $w(t)$ is the spreading width which scales as $w(t) \sim t^{\beta}$, with $0 < \beta \leq 1$. The two exponents satisfy the universal relation $\gamma = 1/(1-\beta)$. We demonstrate these results through numerical work on one-dimensional quasiperiodic systems and the three-dimensional Anderson model of disorder. We provide an analytical derivation of these relations by using the memory function formalism of quantum dynamics. Furthermore, we present an application to experimental results for the quantum kicked rotor.

DOI: 10.1103/PhysRevLett.86.2485 PACS numbers: 03.65.–w, 02.40.Xx, 71.23.Ft, 71.30.+h

Transport in quantum systems exhibits a variety of different behaviors ranging from ballistic motion to diffusion, and to localization. In between also lies the more exotic type known as anomalous diffusion, where a wave packet spreads slower than a linear function of time for ballistic motion, but not proportional to the square root of time as in the normal diffusive case. Anomalous diffusion has been found theoretically in quasicrystal models [1–7], in two-dimensional (2D) lattices in magnetic fields [2,3,6,8], and at metal-insulator transitions in disordered systems [9]. Previous work has been mainly focused on the analysis of the temporal decay of the survival probability at the initial position and the growth of the wave packet width. The time-averaged survival probability typically decays as $t^{-\delta}$ at large times with $0 < \delta \leq 1$, where the exponent has been shown to be given by the fractal dimension of the local density of states [3,6]. On the other hand, the width of a wave packet grows as t^{β} with $0 < \beta \leq 1$, where the exponent depends not only on the energy spectrum [2,5,10] but also on the fractal characteristics of the eigenwave functions [4].

In this Letter, we focus on the spatial form of wave packets in quantum diffusion, and establish a universal relationship between the front shape and the time dependence of the width of a spreading wave packet. We find that, at long times, the front of a wave packet becomes time invariant after scaling in width $w(t)$ and height $A(t)$. Moreover, the probability distribution in the tail regions is described to a high accuracy by the stretched exponential,

$$P(x,t) = A\exp(-|x/w|^{\gamma}), \tag{1}$$

where the exponent is time independent with $1 < \gamma < \infty$. Furthermore, we reveal a universal relationship,

$$\gamma = 1/(1-\beta), \tag{2}$$

between the shape exponent γ and the diffusion exponent β as defined by $w(t) \sim t^{\beta}$. We demonstrate these results through numerical work on the Fibonacci chain and the 3D Anderson model, and present an application to experimental results for the quantum kicked rotor. We also provide an analytical derivation of Eqs. (1) and (2) using the memory function formalism of quantum dynamics.

The spreading of a wave packet in a quantum system is governed by the Schrödinger equation, which for tight-binding models has the form $i\dot{\psi}(n,t) = V(n)\psi(n,t) + \sum_{n'} h(n,n')\psi(n',t)$, where $\psi(n,t)$ is the wave function amplitude at position n at time t, $V(n)$ is the on-site potential, and $h(n,n')$ are the nearest-neighbor hopping

integrals. The initial condition is chosen to be a wave function localized at a single site. For a given potential $V(n)$, the probability distribution $P(n,t) = |\psi(n,t)|^2$ can be obtained either by integrating the Schrödinger equation directly or by expanding in terms of the eigenstates.

We start with the Fibonacci chain, a 1D model of quasicrystals [11,12]. The hopping integrals take the form $h(x,x') \equiv 1$ (here x and x' are integers) and the on-site potential takes two values $a = -V$ and $b = V$ arranged according to the Fibonacci sequence, $abaababa\ldots$, which can be constructed from a by iterating the inflation rule ($a \rightarrow ab, b \rightarrow a$). In Fig. 1, we present the semilog plot of $P(x,t)$ versus x at $t = 500$ with different values of V. The width of the wave packet depends strongly on the potential strength with the widest corresponding to the ballistic case $V = 0$ and the narrowest corresponding to the largest V. Moreover, they have different shapes ranging for boxlike to wedgelike.

The wave packet can be well fitted to the stretched exponential of the form in Eq. (1). In Figs. 2(a)–(f), we present the scaled probability distribution $P(x,t)/A$ as a function of x/w at different times for each V. Values of A and w were obtained by fitting (the standard mean square fit) the raw data of $P(x,t)$ to a stretched exponential with $\gamma = 7.69, 3.13, 2.0, 1.67, 1.47$, and 1.33 from Figs. 2(a) to 2(f). We clearly see that, after scaling $P(x,t)$ in width and in height by using its fitting parameters w and A, the wave packet at different times overlap together in each panel, indicating that the scaled front shape is invariant in time. We note that such a good fit holds over 30 orders of magnitude up to the precision limit of the simulation. This result provides unambiguous evidence that the front shape of a wave packet is well defined and follows the description of the stretched exponential.

More surprisingly, we find that the shape exponent γ is completely specified by the diffusion exponent β. The power-law time dependence of the width $w(t) \sim t^{\beta}$ can be seen in Fig. 3 from the straight lines in the log-log plot of w versus t, where the slopes give $\beta = 0.87, 0.68, 0.50, 0.40, 0.32$, and 0.25 for various values of the potential $V = 0.5, 1.0, 1.65, 3.0, 5.0$, and 10.0, respectively. These values of β are indistinguishable from those obtained from calculations of the second moment [1]. We show in the inset the correlation between β and γ, which is found to be well described by the simple formula Eq. (2). Therefore, the normal diffusive case $\beta = \frac{1}{2}$ has a Gaussian wave packet similar to the classical behavior. On the superdiffusive side ($\beta > \frac{1}{2}$) and towards the ballistic limit ($\beta = 1$), the distribution becomes flatter on the top and steeper at the edges; while on the subdiffusive side ($\beta < \frac{1}{2}$) and towards the localization limit ($\beta = 0$), the wave packet becomes sharper in the middle and more ramped in the tails.

The same results have been found not only for other 1D systems, such as the silver-mean quasiperiodic chain [13], the Harper model [14,15], and the random dimmer model [16], but also for higher dimensional systems such as the 3D Anderson model at the critical disorder of the metal-insulator transition. In the Anderson model, the site energies $V(n)$ are uniformly distributed in the interval $-U/2 \leq V(n) \leq U/2$, and the nearest hopping integrals take the form $h(n,n') \equiv 1$. At the transition with $U = 16.5$ [17], electron wave packets display anomalous diffusion with $\beta = \frac{1}{3}$ [9]. Figure 4 shows the probability distributions $P(x,0,0,t)$ at the transition at $t = 1$ for systems of different sizes, each obtained by averaging

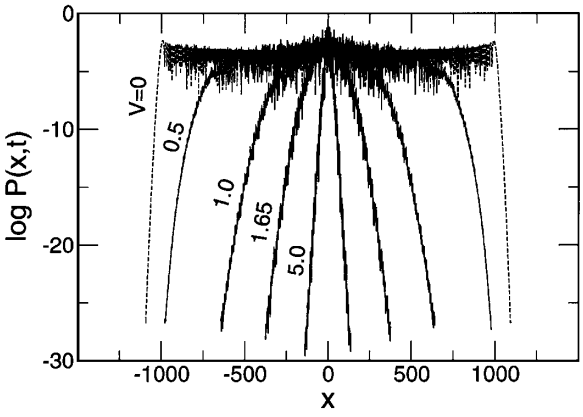

FIG. 1. Semilog plot of $P(x,t)$ versus x at $t = 500$ for the Fibonacci chain with different V.

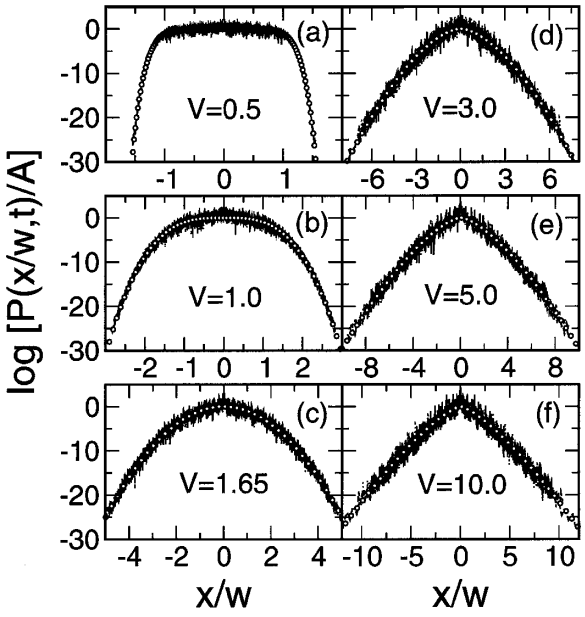

FIG. 2. Semilog plot of the scaled probability distribution $P(x/w,t)/A$ versus x/w at different times (t) for the Fibonacci chain with different V. Lines of wave packets at different t overlay nicely together after scaling, where $t = 100$, 200, 500, and 1000 in (a); $t = 100$, 500, 1000, and 2000 in (b); $t = 100$, 500, 1000, and 5000 in (c); $t = 100$, 1000, 10 000, and 100 000 in (d); $t = 100$, 1000, 10 000, and 100 000 in (e); and $t = 100$, 10 000, 100 000, and 1 000 000 in (f). Open circles from (a) to (f) are fitting results to a stretched exponential with $\gamma = 7.69$, 3.13, 2.0, 1.67, 1.47, and 1.33, respectively.

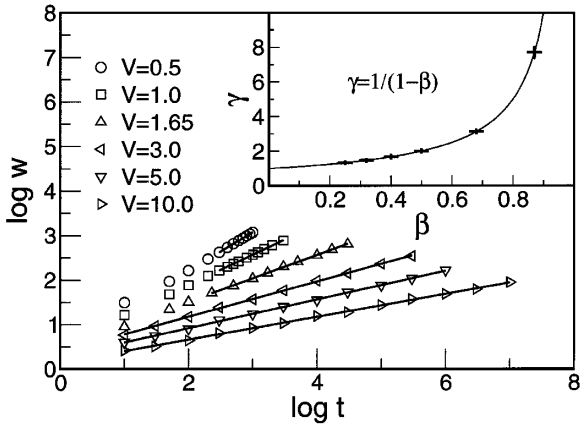

FIG. 3. The scaling behavior of the spreading width $w(t) \sim t^{\beta}$ in a Fibonacci chain with different V. The linear fit (solid lines) gives $\beta = 0.87$, 0.68, 0.50, 0.40, 0.32, and 0.25 for $V = 0.5$, 1.0, 1.65, 3.0, 5.0, and 10.0, respectively. Inset shows the relation between exponents γ and β with error bars indicated.

100 different disorder configurations. As expected from Eq. (2), the front shape shown in Fig. 4 is well described by the stretched exponential with $\gamma = 1.5$. In addition, we found $\gamma = 2$ in the metallic regime ($U < 16.5$) for normal diffusion and $\gamma = 1$ in the insulator regime ($U > 16.5$) for localization.

Equations (1) and (2) provide a useful framework for analyzing experimental results of anomalous diffusion. Experiments have been performed using an atom-optics realization of the quantum kicked rotor, which is known to be described by a 1D quasiperiodic tight-binding model in momentum space; the details of the experiment are described in [18]. In each case that we study, the distributions after 30, 40, 50, 60, and 70 kicks are fit simultaneously to Eq. (1) while imposing Eq. (2) as a constraint. We study three distinct cases, beginning with dynamical localization (with the kick strength $K = 11.2$), where we find an exponent $\gamma = 1.06 \pm 0.19$, which is consistent with exponential localization. In the next case, the wave packets exhibit anomalous diffusion ($K = 8.4$) [18], where the fit yields $\gamma = 1.48 \pm 0.16$; this larger exponent is consistent with the curved, nonexponential distribution tails observed in the experiments [19]. Finally, we study the kicked rotor with $K = 11.2$ driven strongly (200%) by amplitude noise, where the dynamics mimic classical diffusion; in this case, we find $\gamma = 2.03 \pm 0.14$, which is consistent with normal diffusion. We did not attempt to fit the central peaks where the stretched exponential is not expected to apply. The data and fits for all three cases are shown at 70 kicks in Fig. 5, showing excellent agreement in the tails of the distributions.

We have thus demonstrated the universality of the stretched exponential distribution Eq. (1) and the scaling relation Eq. (2), and we now show how they may be derived from the general principles of quantum mechanics. As an exact consequence of Schrödinger's equation and under the initial condition of a diagonal density matrix, the probability distribution follows the generalized master equation (GME) [20],

$$\frac{\partial}{\partial t} P(n,t) = \int_0^t dt' \sum_{n'} W(n,n',t-t') \Delta P(n',n,t') , \tag{3}$$

where $\Delta P(n',n,t') = P(n',t') - P(n,t')$, and $P(n,t)$ is the probability at site n. $W(n,n';t-t')$ is known as the memory function which is related to the off-diagonal terms of the Liouville equation for the density matrix. The GME is non-Markovian, but is causal and has time-translational symmetry. After performing a coarse graining in the position n, the GME still preserves its form [21] but becomes

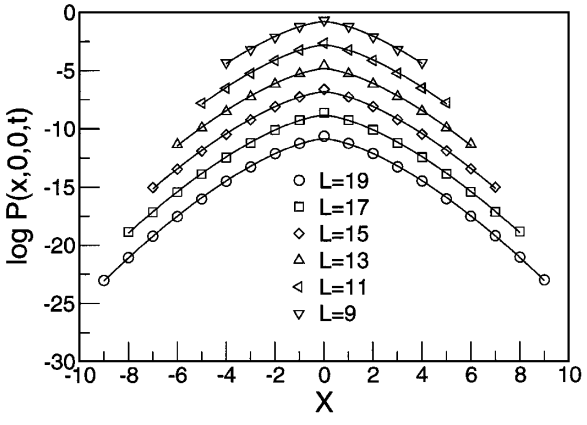

FIG. 4. Semilog plot of the probability distribution $P(x,0,0,t)$ at $t = 1$ at the 3D Anderson transition for different system sizes $L \times L \times L$. Results for $L = 11$, 13, 15, 17, and 19 have been shifted by multiples of -2 for clarity. Lines are the fitting results to a stretched exponential with $\gamma = 1.5$.

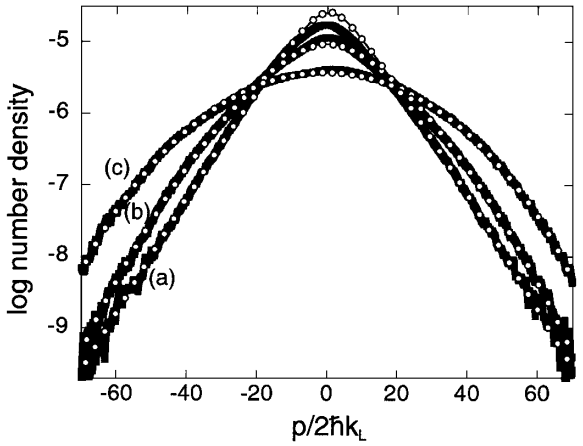

FIG. 5. Experimental quantum kicked rotor data (heavy lines) with best fits (open circles), shown only at the time of 70 kicks for clarity. The three regimes shown are (a) exponential localization, (b) anomalous diffusion, and (c) noise-induced delocalization, for which the respective exponents are $\gamma = 1.06$, 1.48, and 2.03.

translationally invariant due to the statistical homogeneity of the system. Denoting the coarse-grained position by x, we have

$$\frac{\partial}{\partial t} P(x,t) = \int_0^t dt' \sum_{\Delta x} g(\Delta x; t - t') \Delta P(\Delta x, x, t'), \quad (4)$$

where $\Delta P(\Delta x, x, t') = P(x + \Delta x, t') - P(x, t')$. At long times and in the tail regions, the coarse-grained density varies slowly in space, and we may take a gradient expansion of ΔP in Δx. Assuming that $g(\Delta x, t)$ has a finite range in Δx to support this gradient expansion and that the quantum diffusion has no preferred direction, then a Laplace transform of Eq. (4) leads to

$$s\tilde{P}(x,s) = \tilde{I}(s) \frac{\partial^2 \tilde{P}}{\partial x^2}(x,s), \quad (5)$$

with $\tilde{I}(s)$ being the Laplace transform of $I(t) = (\frac{1}{2}) \times \sum_{\Delta x} g(\Delta x; t) (\Delta x)^2$. The solution of Eq. (5) is $\tilde{P}(x,s) = B(s) e^{-|x| f(s)}$, where $f(s) = \sqrt{s/\tilde{I}(s)}$ and $B(s)$ is a normalization constant.

We calculate the probability $P(x,t)$ using the inverse Laplace transform,

$$P(x,t) = \int ds\, B(s) \exp[st - |x| f(s)]. \quad (6)$$

Consistent with the observed anomalous diffusion, we assume now the power-law behavior $f(s) \approx f_0 s^\beta$ as $s \to 0$. Using the stationary phase approximation, which occurs for $s = (\beta f_0 |x|/t)^{1/1-\beta}$, we obtain the leading exponential behavior of the probability as Eq. (1), with a width $w = t^\beta / f_0 \beta^\beta (1 - \beta)^{1-\beta}$ and an exponent γ given by the relation Eq. (2). The above analysis is valid for $t^\beta < |x| < t$, because the stationary point needs to be close to $s = 0$ to be consistent with the long time assumption, and yet the separation needs to be larger than the width of the stationary phase. These inequalities indicate that the stretched exponential is valid beyond the width of the wave packet and within the causal zone of ballistic motion. Our results thus complement the recent finding of $P(x,t) \sim |x|^{D-1}$ for the central part of a wave packet with $|x| < t^\beta$, where D is a multifractal dimension of the eigenstates [4].

This research was supported by the U.S. National Science Foundation under Grants No. DMR-0071893, No. DMR-9705406, and No. PHY-9987706, the Welch Foundation, the U.S. Department of Energy under Contract No. DE-AC05-00OR22725 with the Oak Ridge National Laboratory, managed by UT-Battelle, LLC, the Fannie and John Hertz Foundation, and the National Natural Science Foundation of China.

[1] H. Hiramoto and S. Abe, J. Phys. Soc. Jpn. **57**, 230 (1988).

[2] T. Geisel, R. Ketzmerick, and G. Petschel, Phys. Rev. Lett. **66**, 1651 (1991).

[3] R. Ketzmerick, G. Petschel, and T. Geisel, Phys. Rev. Lett. **69**, 695 (1992).

[4] R. Ketzmerick, K. Kruse, S. Kraut, and T. Geisel, Phys. Rev. Lett. **79**, 1959 (1997).

[5] B. Passaro, C. Sire, and V. G. Benza, Phys. Rev. B **46**, 13 751 (1992); H. Q. Yuan, U. Grimm, P. Repetowicz, and M. Schreiber, Phys. Rev. B **62**, 15 569 (2000); H. Q. Yuan and J. X. Zhong, Acta Phys. Sin. **7**, 196 (1998).

[6] J. X. Zhong and R. Mosseri, J. Phys. Condens. Matter **7**, 8383 (1995).

[7] J. Bellissard, Mater. Sci. Eng. A (to be published); D. Mayou, in *Lectures on Quasicrystals,* edited by F. Hippert and D. Gratias (Les Editions de Physique, Les Ulis, 1994), pp. 417–462; C. Berger, *ibid.,* pp. 463–504; C. Sire, *ibid.,* pp. 505–536.

[8] H. Hiramoto and S. Abe, J. Phys. Soc. Jpn. **57**, 1365 (1988); S. N. Evangelou and D. E. Katsanos, J. Phys. A **26**, L1243 (1993); M. Wilkinson and J. Austin, Phys. Rev. B **50**, 1420 (1994).

[9] T. Ohtsuki and T. Kawarabayashi, J. Phys. Soc. Jpn. **66**, 314 (1996); B. Huckestein and L. Schweitzer, Phys. Rev. Lett. **72**, 713 (1994); T. Terao, Phys. Rev. B **56**, 975 (1997); T. Kawarabayashi and T. Ohtsuki, Phys. Rev. B **53**, 6975 (1996).

[10] I. Guarneri, Europhys. Lett. **10**, 95 (1989); Europhys. Lett. **21**, 729 (1993); F. Piéchon, Phys. Rev. Lett. **76**, 4372 (1996); H. Schulz-Baldes and J. Bellissard, Rev. Math. Phys. **10**, 1 (1998).

[11] M. Kohmoto, L. P. Kadanoff, and C. Tang, Phys. Rev. Lett. **50**, 1870 (1983); S. Ostlund, R. Pandit, D. Rand, H. J. Schellnhuber, and E. D. Siggia, Phys. Rev. Lett. **50**, 1873 (1983).

[12] Q. Niu and F. Nori, Phys. Rev. Lett. **57**, 2057 (1986); Phys. Rev. B **42**, 10 329 (1990).

[13] G. Gumbs and M. K. Ali, Phys. Rev. Lett. **60**, 1081 (1988); M. Holzer, Phys. Rev. B **38**, 1709 (1988); J. X. Zhong, J. R. Yan, and J. Q. You, J. Phys. A **24**, L949 (1991).

[14] P. G. Harper, Proc. Phys. Soc. London Sect. A **68**, 874 (1955); Azbell M. Ya, Soc. Phys.-JETP **19**, 634 (1964); D. R. Hofstadter, Phys. Rev. B **14**, 2239 (1976); S. Aubry and G. Andre, Ann. Isr. Phys. Soc. **3**, 133 (1980).

[15] The Harper model displays a metal-insulator transition. We found ($\gamma \to \infty, \beta = 1$) and ($\gamma = 1, \beta = 0$) in the metallic and insulator regimes, respectively. At the transition, wave packets show multiscaling behavior in the sense that the widths defined through different moments of the wave packet, $w_m = \langle |x|^m \rangle^{1/m}$, can have different exponents in their power-law time dependence $w_m \sim t^{\beta_m}$ [4]. The exponents range from 0.46 at $m = 1$ to 0.52 for high moments, where the latter heavily emphasize on the extreme tails of the wave packet. As expected, we found $\beta = 0.52$ for the width of the front and $\gamma = 1/(1 - \beta) = 2.10$ for its shape.

[16] D. H. Dunlap, H. L. Wu, and P. W. Phillips, Phys. Rev. Lett. **65**, 88 (1990). In this system, states in most of the spectrum are exponentially localized, yet there are bands where states are extended. A wave packet in such a system will spread with ballistic tails due to extended states superposed with a strong peak in the middle due to localized and less mobile states. When the wave packet is restricted to a

spectral region where the wave functions have similar behaviors, our formula can give an accurate fit to the entire wave packet.

[17] H. Grussback and M. Schreiber, Phys. Rev. B **51**, 663 (1995), and references therein.

[18] D. A. Steck, V. Milner, W. H. Oskay, and M. G. Raizen, Phys. Rev. E **62**, 3461 (2000).

[19] B. G. Klappauf, W. H. Oskay, D. A. Steck, and M. G. Raizen, Phys. Rev. Lett. **81**, 4044 (1998).

[20] V. M. Kenkre, in *Exciton Dynamics in Molecular Crystals and Aggregates,* edited by G. Höhler, Springer Tracts in Modern Physics Vol. 94 (Springer-Verlag, Berlin, 1982), p. 1.

[21] This is true when the initial condition is also coarse grained, which is the case because we do make averages over the initial positions.